Revealing the effect of X-ray or proton brain irradiation on systemic inflammation and leukocyte subpopulation interplay in rodents

Thao-Nguyen Pham, Julie Coupey, Marc Rousseau, Juliette Thariat, Samuel Valable

Title: Revealing the effect of X-ray or proton brain irradiation on systemic inflammation and leukocyte subpopulation interplay in rodents

Authors names and affiliations

Thao-Nguyen Pham[1,2], Julie Coupey[1], Marc Rousseau[2], Juliette Thariat[2,3]*, Samuel Valable[1]*

[1]Université de Caen Normandie, CNRS, Normandie Université, ISTCT UMR6030, GIP CYCERON, F-14000 Caen, France

[2]Laboratoire de physique corpusculaire UMR6534 IN2P3/ENSICAEN, France - Normandie Université, France

[3]Department of Radiation Oncology, Centre François Baclesse, Caen, Normandy, France

*Authors equally contributed/Corresponding authors

Corresponding authors

Samuel Valable, PhD

ISTCT Laboratory, UMR 6030, Bd H Becquerel, BP 5229, 14074 Caen Cedex

samuel.valable@cnrs.fr

Juliette Thariat, MD, PhD

LPC Laboratory, UMR6534, Bd Maréchal Juin, 14000 Caen

jthariat@gmail.com

Conflicts of Interest:

None.

Abstract

The absolute lymphocyte count (ALC), lymphocyte-to-monocyte ratio (LMR), and neutrophil-to-lymphocyte ratio (NLR) offer convenient means to assess systemic inflammation post-cancer treatment, which influences treatment outcomes. Understanding these biomarker variations and leukocyte subpopulation interplay is crucial for optimizing radiotherapy. Herein, leukocyte subpopulations (T-CD4+, T-CD8+, B-cells, NK-cells, neutrophils, monocytes) during and after brain irradiation (using X-rays or Protons) in tumor-free mice were used to compute ALC, LMR, and NLR, on which radiation parameter influence was assessed by principal component analysis (PCA). NLR kinetics were further examined using modeling. Leukocyte subpopulations interplays and their response to radiation parameters were examined using PCA and correlation analysis. Under X-rays, ALC and LMR decreased, with ALC recovered to baseline after irradiation, but not LMR. Both X-rays and protons increased the NLR during irradiation, recovering in protons but not X-rays. Both irradiation volume and dose rate had a pronounced effect on the NLR. Leukocyte subpopulation interplay was observed under X-rays and protons, normalizing in the proton group by day 28. Lymphopenia was observed in all lymphocyte subpopulations under X-ray irradiation but not protons. The recovery patterns varied among the subpopulations. Neutrophil counts increased during irradiation, with the recovery of protons, but not X-rays, by day 28. Interplays between NK-cells and myeloid subpopulations were evident under X-rays but not protons. Importantly, no interplay was detected between myeloid cells and T/B-cells, indicating that LMR and NLR variations were primarily due to independent responses to brain irradiation. A tumor-free experimental mouse model was used to study the effects of brain radiotherapy on systemic immunity. When administering fractionated irradiation with a total dose of 20 Gy using a vertical beam to either the whole brain or hemi-brain, proton irradiation had fewer adverse impacts on the immune system compared to X-rays in tumor-free rodents.

Summary sentence

Under fractionated irradiation with a total dose of 20 Gy delivered by a vertical beam to either the whole brain or hemi-brain, proton irradiation induces fewer adverse effects on the immune system compared to X-rays in tumor-free rodents.

Keywords: radiotherapy, immune response, brain irradiation, leukocyte subpopulations, neutrophil-to-lymphocyte ratio, proton therapy

1 Background

Over the past decade, it has become evident that persistent systemic inflammation is closely linked to unfavorable outcomes in numerous solid malignancies [1]. Inflammation is difficult to measure and it is associated with poor prognosis in cancer treatment. Inflammation can be roughly estimated using the neutrophil-to-lymphocyte ratio (NLR) [2]. The NLR has been extensively studied as a prognostic marker in patients with solid tumors because it reflects the inflammatory response to cancer [3]. The NLR has also been used for the stratification of numerous cancers and is correlated with tumor size, stage, metastatic potential, and lymphatic invasion [4,5]. Several studies have reported associations between survival rates and the NLR, which is a representative marker of tumor immunity [5–7]. In the context of brain tumor treatment, the dynamic change in the NLR during radiochemotherapy has been shown to be a good prognostic factor in the treatment of glioblastoma and is more significant than the changes in the neutrophil and total lymphocyte counts [8]. In addition to the NLR, other inflammatory markers based on leukocytes, such as the absolute lymphocyte count (ALC) and lymphocyte–monocyte ratio (LMR), are clinically significant for assessing the impact of the inflammatory response on the prognosis of various solid tumors, including colorectal, gastric, and lung cancers [9]. These leukocyte-based inflammatory biomarkers are of particular interest because of their accessibility and ease of computation based on routine blood cell counts. Among these biomarkers, the ALC and NLR have frequently been studied as prognostic indicators for radiotherapy.

Despite these advances, the precise mechanisms underlying leukocyte changes in response to radiotherapy remain unknown. Immune cells, especially lymphocytes, are among the most radiosensitive cells in the human body [10]. A common side effect of radiotherapy is the development of radiation-induced lymphopenia (RIL) [11]. RIL is characterized by the rapid depletion of circulating lymphocytes following irradiation and can be both profound and long-lasting. This condition affects more than 40% of patients undergoing radiotherapy for solid tumors, including brain tumors [12]. RIL has emerged as a robust adverse prognostic factor for patient outcomes, whether in the context of radiotherapy alone or in combination with radioimmunotherapy [13]. Moreover, the recovery of immunocompetence following periods of hematopoietic injury is vital not only for effective responses to pathogens and tumor antigens but also for optimal responses to cancer immunotherapy [14]. In contrast, the expansion of myeloid populations (such as neutrophils and monocytes) following radiation treatment has been found to be correlated with RIL and negatively correlated with the prognosis of cancer treatment. The balance between myeloid and lymphoid populations is critical for immune activity. A skewed myeloid-to-lymphoid balance, as indicated by the

NLR and LMR, signifies immune stimulation and inflammation [15,16]. During inflammation, interactions between myeloid and lymphoid populations contribute to the interplay between innate and adaptive immune responses. However, it remains unclear whether such interactions occur directly after radiotherapy [15].

Recent advances in radiotherapy have led to the development of new irradiation methods. The choice between X-ray and particle therapy may modify leukocyte subpopulations in the blood and alter the immunological effects of radiotherapy. For example, proton therapy has been reported to reduce the severe lymphopenia rate by 50% compared with X-ray radiotherapy in patients undergoing radiochemotherapy for esophageal carcinoma [17]. This difference was attributed to the lower doses delivered to critical organs at risk (body, spleen, liver, lungs, and heart) with proton therapy than with X-ray therapy [18]. Additionally, proton therapy was found to decrease the volume of the brain exposed to radiation and the likelihood of lymphopenia in glioblastoma patients undergoing radiochemotherapy [19].

Understanding how radiation parameters affect ALC, LMR, NLR, and the dynamics of leukocyte subpopulations is essential for optimizing radiotherapy treatments and their combination with immunotherapies. This study aimed to analyze the impact of brain irradiation using various radiation modalities on circulating leukocyte-based inflammatory biomarkers and the interplay between leukocyte subpopulations using a combination of computational methods.

2 Methods

2.1 Data

This study utilized data from two preclinical experiments that investigated the effects of brain radiation on the immune population of healthy seven-week-old C57BL/6 female mice (16–20 g; Janvier Labs) [20]. The animal experiments were performed in accordance with current European regulations, with permission from the Regional Committee on Animal Ethics, CENOMEXA, for the experiments carried out in Caen (#27343) and CEEA035 for those performed in Strasbourg (#27413). All animals were genetically identical; thus, no blinding or randomization was performed to select irradiated and control mice. Daily surveillance and body weight follow-up were performed twice per week.

Physical doses of 2.5 Gy per fraction in four fractions were delivered to the brain vertically on two consecutive days using either X-ray (XRad-225Cx, Cyceron, Caen, France) or proton (PRECy platform, CYRCé cyclotron, Strasbourg, France) beams. The dose applied to the brain was previously described [21]. Mice were irradiated under anesthesia

(1 L/min with 5% isoflurane for induction and 2% for maintenance in 70% N_2O/30% O_2). Irradiation was performed using a square (L=1 cm)/rectangular (L=1 cm; l=0.5 cm) collimator. For X-rays, the brain was located using an on-board CT scan. For protons, the energy of the proton beam was set to 25 MeV to accurately target the brain (Gaussian distribution with an average value of 24.85 MeV with a standard deviation of 127 keV) [22]. To obtain a flat transverse dose profile, we used a 100-micron thick Al-scattering foil 340 cm upstream from the end of the beam line and to extract the beam from vacuum to air, it passes through a second 50-micron Al foil (4-5 cm before the target). Then we utilized a rotating wheel composed of 20 different thicknesses of aluminum foil as degrader to modulate the energy, thus managing the Spread-Out Bragg Peak (SOBP) [22]. The anesthetized mice were placed in a neck cradle. A laser pointer was used to calibrate the irradiated brain center and spare the olfactory bulbs, skull base nodes, and brainstem.

Blood samples were collected at two time points: during irradiation on day 2 and after the final radiation fraction on day 28. Flow cytometry was used to quantify the blood concentrations of different leukocyte subpopulations, including T CD4+ cells, T CD8+ cells, B cells, and NK cells from the lymphoid population and neutrophils and monocytes from the myeloid population. The experimental conditions included different types of radiation beams (X-rays or protons), irradiated volumes (whole brain or left hemisphere), and dose rates (1 or 2 Gy/min). Non-irradiated mice were used as controls. The full detailed experimental protocol for mouse irradiation, blood collection, flow cytometry and gating strategy are presented in the supplementary material section 1 and in Coupey et al. 2024 [20].

To standardize the data, the concentration of each cell population was normalized to the ratio of the control group in each experiment using the baseline concentration as a reference fixed at a value of 1. Figure 1 illustrates the variations in leukocyte subpopulations during irradiation on day two and after irradiation on day 28. T cells (CD4+ and CD8+) and B cells exhibited a significant reduction in cell count during irradiation, with subsequent recovery within one month of irradiation. In contrast, there was a significant reduction in the percentage of NK cells, which persisted even one month after irradiation. However, the number of neutrophils increased in more than 50% of the mice during irradiation, and this increase continued to be evident on day 28. Compared with those in the control group, the number of monocytes in the treated group did not significantly change. Notably, there was greater variability in leukocyte counts postirradiation in the irradiated group than in the control group, indicating the presence of distinct immune response subgroups following irradiation.

(Figure 1)

2.2 Leukocyte-based inflammatory biomarkers

The absolute lymphocyte count (ALC), neutrophil–lymphocyte ratio (NLR) and lymphocyte–monocyte ratio (LMR) were calculated as follows:

$$ALC_i = C^i_{T-cells} + C^i_{B-cells} + C^i_{NK-cells}$$

$$NLR_i = \frac{C^i_{Neutrophils}}{ALC_i}; LMR_i = \frac{ALC_i}{C^i_{Monocyte}}$$

where ALC_i, NLR_i, LMR_i are the ALC, NLR, and LMR at time i; $C^i_{T-cells}$, $C^i_{B-cells}$, $C^i_{NK-cells}$, $C^i_{Neutrophils}$, and $C^i_{Monocyte}$ are the concentrations of T cells, B cells, NK cells, neutrophils, and monocytes at time i, respectively.

The ALC, LMR, and NLR were normalized to the ratio of the control group in each experiment, with the reference baseline concentration fixed at 1. Statistical analyses were performed using RStudio version 4.1.2. The Mann–Whitney U test (Wilcoxon test) was applied to test whether there was a difference in ALC, LMR, and NLR variations under brain irradiation between the irradiated and non-irradiated groups under the null hypothesis that the ALC, LMR, and NLR values were the same between the irradiated and control groups. The summary of all parameters used in the analysis was mentioned in Table 1.

2.3 Impact of radiation parameters on leukocyte-based inflammatory biomarkers

Exploratory data analysis

The correlations between ALC, NLR, and LMR during and after irradiation were assessed. Principal component analysis (PCA) was then applied to summarize the influence of radiation parameters on the ALC, NLR or LMR during and after irradiation. The radiation parameters included the irradiation type employed (X-rays or protons), irradiated volume (whole brain or hemi-brain), and dose rate (1 or 2 Gy/min).

Clustering NLR data into subgroups

To discern the existence of subgroups within NLR kinetics and their distribution in response to specific radiation conditions (irradiation type: X-rays or protons; irradiated volume: whole brain or hemi-brain; dose rate: 1 Gy/min or 2 Gy/min), longitudinal mixture modeling was performed. This clustering process was executed using the FlexMix package version 2.4.1 (20), with the Akaike information criterion (AIC) used as the criterion to identify the optimal number of clusters. The order of the polynomial model was selected between the 1st-, 2nd-, and 3rd-order polynomial

models based on the mean square error (MSE). The outcomes derived from longitudinal mixture modeling facilitated the identification of NLR kinetic subgroups based on common kinetic trends.

Tree-based modeling

A tree-based modeling approach was adopted to explore the hierarchical relationships between radiation parameters and NLR subgroups. A decision tree was constructed by minimizing the MSE during the node-splitting process, wherein the strategy sought to minimize the MSE.

The splitting process terminated when no further splitting was observed. A post-pruning process was performed to remove non-significant branches. The analytical approach was executed using the *rpart* package version 4.1.19.

2.4 Leukocyte subpopulation interplay during and after irradiation

Leukocyte subpopulations were clustered into distinct groups based on cell count patterns during irradiation. Clustering was determined by calculating Pearson correlation coefficients and employing the k-means clustering algorithm. The results of this analysis are presented in the form of a heatmap, and hierarchical clustering was applied using the *pheatmap* package version 1.0.12 [23]. Correlations were examined at two specific time points: during irradiation on day two and after irradiation on day 28.

PCA was applied to provide a summary and visual representation of the six leukocyte subpopulations during irradiation (day 2) and post-irradiation (day 28). This analysis allowed us to project the data onto a two-dimensional graph. In addition to leukocyte subpopulations, the supplementary parameters included three radiation-related factors: irradiation type, irradiation volume, and dose rate. PCA was performed using the *FactoMineR* package (for the analysis) and *factoextra* package (for data visualization) in R software [24].

3 Results

3.1 Impact of brain irradiation on leukocyte kinetics

Brain irradiation induced a significant reduction in the ALC and LMR on day 2, which demonstrated complete recovery by day 28. Conversely, the NLR increased during irradiation on day 2 (Figure 2A1), with no subsequent recovery observed after irradiation on day 28 (Figure 2A2). There was no significant correlation between the LMR during or after irradiation (Figure 2B1 and 2). Conversely, the ALC and NLR during irradiation were significantly correlated with

the ALC and NLR after irradiation (Figure 2B3). PCA was then applied to elucidate the variability in ALC, LMR, and NLR during and after brain irradiation (Figure 2C).

(Figure 2)

For both ALC and LMR, the primary principal component accounted for 56.6% of the data variance, whereas the second principal component accounted for 43.3%. Given the nearly equal contributions of both principal components to the data variance, it can be inferred that variations in ALC or LMR during irradiation were not strongly associated with variations in ALC or LMR after irradiation. The first component showed elevated ALC and LMR levels during and after irradiation. The second component indicated elevated levels of ALC or LMR during irradiation and diminished levels after irradiation. For ALC, the control (non-irradiated) group and protons exhibited positive correlations with both components. Conversely, X-rays and a dose rate of 1 Gy/min were negatively correlated with both components. Whole-brain irradiation displayed a negative correlation with the first component, whereas a dose rate of 2 Gy/min and hemi-brain irradiation showed a minimal correlation with both components. These findings suggest that the use of X-ray irradiation at a lower dose rate and with a larger irradiation volume is associated with lower lymphocyte counts during irradiation. The recovery of lymphocyte levels after irradiation was influenced by the irradiated volume, with smaller volumes showing better recovery. The recovery of lymphocyte levels after irradiation was influenced by the irradiated volume, with smaller volumes showing better recovery.

The primary principal component explained 71% of the variance in the NLR, while the second principal component accounted for 29%. Both the NLR during and after irradiation exhibited strong positive associations with the major components. The first component denoted heightened NLR levels during and after irradiation, whereas the second component indicated low NLR levels during irradiation and elevated NLR levels after irradiation. The control group exhibited a negative correlation with the first component, whereas whole-brain irradiation displayed a positive correlation with the first component, with hemi-brain irradiation resembling the behavior of the control group. A dose rate of 1 Gy/min exhibited a negative correlation with the second component, whereas a dose rate of 2 Gy/min displayed minimal correlation with both components. The first component represents the effect of the irradiated volume, and the second component represents the dose rate. X-rays demonstrated a positive correlation, and protons exhibited a negative correlation with both components. This suggests that both X-rays and protons induced an increase in the NLR during irradiation, with this increase being more pronounced with larger irradiation volumes

and lower dose rates. The recovery of the NLR after irradiation was observed for protons but not for X-rays, and higher dose rates led to better recovery after 28 days.

Hence, the radiation type of X-rays or protons is an important parameter for ALC, LMR, and NLR variations. These variations, stratified by irradiation type, are shown in Figure 3. Compared with those in the control group, the ALC and NLR in the X-ray irradiation group were significantly lower (Figure 3A.1). However, the reduction in the LMR during irradiation did not reach statistical significance. The ALC fully recovered to baseline levels after irradiation (Figure 3A.2). Conversely, the NLR remained elevated even after irradiation, with 75% of X-ray-treated mice exhibiting NLR values greater than those in the control group (Figure 3A.2). Notably, no statistically significant changes were observed in the ALC, LMR, or NLR during proton irradiation. Nevertheless, more than 50% of the mice exhibited NLR values exceeding the baseline, and more than 50% displayed LMR values lower than the baseline (Figure 3C.1). This change was reversed for the NLR but not for the LMR after 28 days (Figure 3C.2). In summary, ALC reduction was observed in response to X-rays but not to protons. The LMR and NLR exhibited similar trends under both X-ray and proton irradiation but to a lesser extent under proton irradiation than under X-ray irradiation. These findings suggest that both lymphoid and myeloid cells contribute to the systemic inflammatory response during X-ray irradiation, whereas only myeloid cells are involved in the response to proton irradiation. NLR recovery was observed for protons but not for X-rays, while the LMR remained consistent between the early and late phases post-irradiation.

(Figure 3)

3.2 Neutrophil-to-lymphocyte kinetics following brain irradiation

Given the association between the NLR during and after irradiation, as revealed by PCA (Figure 2B), a more detailed analysis of NLR kinetics was performed using a mixture model. The 2nd-order polynomial model was chosen because it resulted in a lower MSE than the 1^{st-} and 3rd-order models. This approach resulted in the classification of NLR kinetics into 5 distinct clusters. These five clusters were subsequently regrouped into three categories based on their patterns (Figure 4A; for details, see the supplementary figure 1 and supplementary figure 2).

1. Group 1, which included cluster 2, was characterized by stable NLR values over time.
2. Group 2 included clusters 1 and 3, in which the NLR increased during irradiation and gradually decreased (recovered) over time.

3. Group 3, consisting of clusters 4 and 5, exhibited an increase in the NLR during irradiation, followed by recovery and a subsequent late increase on day 28.

Quantitative assessment using a tree-based separation method (Figure 4B) further confirmed that the primary factor influencing NLR kinetics was the irradiation type used, followed by the irradiated volume and dose rate in the X-ray arm. In the case of X-ray irradiation, only 20% of the mice displayed stable NLR kinetics following whole-brain irradiation, whereas 45% exhibited stable NLR kinetics after hemi-brain irradiation. Under X-ray hemi-brain irradiation, a dose rate of 2 Gy/min led to a greater incidence of late increases in NLR kinetics than did a dose rate of 1 Gy/min. In contrast, under proton irradiation, 70% of the mice exhibited stable NLR kinetics. The observed differences in NLR kinetics between X-ray and proton irradiation were statistically significant, as determined by Fisher's exact test ($p = 0.004$, see Figure 4C). No significant difference in NLR kinetics was observed when different irradiated volumes (whole-brain or hemi-brain) or dose rates (1 or 2 Gy/min) were applied (Figure 4D, E).

(Figure 4)

3.3 X-rays and protons have different impacts on the interplay of leukocyte subpopulations

PCA revealed that the variance within the six leukocyte subpopulations could be effectively captured within a two-dimensional plane, accounting for approximately 70% of the variance both during and after irradiation (Figure 5).

On day 2, regarding the leukocyte subpopulations during irradiation, the first principal component accounted for 54.7% of the variance, whereas the second principal component explained 25.5% of the variance (Figure 5A). The first principal component was positively correlated with variations in lymphoid subpopulations (T CD4+, T CD8+, B, and NK cells). Conversely, the second principal component exhibited a positive correlation with variations in myeloid cell subpopulations (neutrophils and monocytes). This implies that the first principal component characterizes the variation in lymphoid subpopulations, whereas the second principal component characterizes the variation in myeloid subpopulations during irradiation. The first principal component exhibited a negative correlation with X-rays and a positive correlation with protons, with the latter exhibiting a stronger correlation than that of the control group.

On day 28, regarding the leukocyte subpopulations post-irradiation, the first principal component accounted for 44.6% of the variance, whereas the second principal component accounted for 29.3% (Figure 5B). The first principal component demonstrated a positive correlation with variations in T and B cells, whereas the second principal component showed a positive correlation with myeloid subpopulations (neutrophils and monocytes) and a negative

correlation with NK cell variation. This suggests that the first principal component characterizes changes in leukocyte populations associated with adaptive immunity, whereas the second principal component describes changes in leukocyte populations associated with innate immunity. X-rays exhibited a positive correlation with the second principal component, whereas proton irradiation exhibited a negative correlation with the second principal component, demonstrating a stronger correlation than in the control group.

These findings suggest that lymphoid subpopulations mount an early response following irradiation, with distinct responses observed in relation to X-rays but not proton irradiation. Although the reduction in lymphoid subpopulation levels induced by X-ray exposure can be reversed, this is not the case for NK cells. Conversely, brain irradiation has a delayed effect on myeloid subpopulations, with an expansion observed specifically in response to X-ray exposure but not proton irradiation.

The lymphocyte subpopulations exhibited divergent responses to radiation exposure. T CD4+, T CD8+, and B cells demonstrated similar response patterns during irradiation, which was marked by a negative correlation with X-ray exposure. These correlations diminished post-irradiation on day 28 and exhibited disparities between T cells (CD4+ and CD8+) and B cells. Notably, the number of B cells after irradiation appeared to be independent of the type of irradiation (Figure 5B). Conversely, NK cell levels were negatively correlated with X-rays and positively correlated with proton irradiation during and after irradiation. These observations suggest that X-ray radiation causes acute lymphopenia across all lymphocyte subpopulations, with full recovery observed within 28 days for B cells, partial recovery of T cells (CD4+ and CD8+), and no recovery of NK cells. Protons exerted minimal influence on lymphoid cell subpopulations.

Neutrophils and monocytes showed a strong correlation with myeloid cell subpopulations. Variations in these subpopulations during irradiation appeared to be largely independent of X-ray exposure and exhibited a more pronounced positive correlation with protons than with X-rays (Figure 5A). After irradiation, the variation was positively correlated with X-rays and negatively correlated with protons (Figure 5B). This suggests an early effect of proton irradiation and a delayed effect of X-ray irradiation on myeloid subpopulations.

(Figure 5)

The data were subsequently stratified based on the irradiation type and subjected to correlation analysis and PCA (Figure 6). X-rays and protons induced distinct correlations among leukocyte subpopulations during brain irradiation.

For both X-rays and protons, leukocyte subpopulations can be effectively categorized into two distinct clusters based on their correlated responses during irradiation.

Under X-ray irradiation, these two groups consisted of (1) T CD4+, T CD8+, and cells and (2) NK cells, neutrophils, and monocytes (Figure 6A, supplementary figure 3). During irradiation on day 2, PCA revealed two primary components, PC1 and PC2, which accounted for 51.6% and 22.4% of the variance in the data, respectively. PC1 exhibited a positive correlation with all leukocyte subpopulations, indicating a general immune response. PC2 was positively correlated with T and B cells but negatively correlated with other subpopulations, suggesting a unique response in these lymphoid cells. Compared with hemi-brain irradiation, whole-brain irradiation was positively correlated with PC1 but negatively correlated with PC2. This indicated that larger irradiated volumes led to greater expansion of myeloid and NK cells, regardless of dose-rate effects, which appeared to be less relevant. After irradiation on day 28, PC1 and PC2 explained 52% and 20.6% of the variance, respectively (Figure 6B, supplementary figure 4). PC1 maintained a positive correlation with all leukocyte subpopulations except for NK cells. PC2 was positively correlated with lymphoid cell subpopulations and negatively correlated with myeloid cell subpopulations. Whole-brain irradiation was negatively correlated with both components, whereas hemi-brain irradiation exhibited positive correlations with both components, suggesting that larger irradiated volumes resulted in lower T and B cell levels post-irradiation, possibly due to slower recovery rates or changes in homeostatic levels. Additionally, a third component, PC3 (15.2% of the variance in the data; see the supplementary information), was strongly correlated with NK cells and increased irradiated volume, indicating that larger irradiated volumes might lead to higher NK cell concentrations (less NK lymphopenia) in the blood post-irradiation.

Conversely, under proton irradiation, the two distinct groups comprised (1) TCD4+, TCD8+, B cells, and NK cells and (2) neutrophils and monocytes (Figure 6C, supplementary figure 5). On day 2 of irradiation, PCA revealed two significant components. PC1 (49.7%) was positively correlated with all lymphoid subpopulations, whereas PC2 (27.2%) was positively correlated with all myeloid subpopulations. In terms of irradiated volume, whole-brain irradiation showed a positive correlation with PC1 and a negative correlation with PC2 (in contrast to hemi-brain irradiation). This suggests that a larger irradiated volume leads to the expansion of myeloid cells and lower levels of lymphoid cells. Regarding the dose rate, 1 Gy/min was positively correlated with PC2 and negatively correlated with PC1 (inversely correlated with 2 Gy/min). This indicates that a lower dose rate is associated with smaller lymphoid subpopulations and higher myeloid cell counts, potentially resulting in a greater NLR and a lower ALC and LMR.

Additionally, PC3 (15% data variance; for details, see supplementary figure 4) was strongly correlated with NK cells, with an increased irradiation volume positively affecting this component. The dose rate had a lesser effect on PC3 cells. After irradiation on day 28, PCA demonstrated that PC1 (56.3%) was positively correlated with all lymphoid subpopulations, whereas PC2 (28.3%) was positively correlated with all myeloid subpopulations (Figure 6D, supplementary figure 6). Whole-brain irradiation was negatively correlated with PC1, whereas hemi-brain irradiation was positively correlated with PC1. The irradiated volume did not significantly correlate with PC2. This suggests that larger irradiation volumes result in fewer lymphoid subpopulations after irradiation. In terms of the dose rate, 1 Gy/min was positively correlated with PC1 and inversely correlated with PC2. This indicated that a lower dose led to higher lymphoid subpopulation levels. Neither the irradiation volume nor the dose rate had a long-term impact on the myeloid subpopulations.

(Figure 6)

4 Discussion

Our study provides information regarding the complex relationship between brain irradiation and inflammation, particularly in the context of the immune response to X-rays and proton therapy.

Our findings indicate that X-ray irradiation led to a uniform degree of lymphopenia in all lymphocyte subpopulations. T cells (CD4+ and CD8+) and B cells displayed varying recovery patterns within 28 days post-irradiation. Conversely, NK cells demonstrate limited capacity for recovery within the same timeframe. In fact, lymphopenia is a well-documented consequence of RT. The severity of lymphopenia is closely linked to the administered dose [25,26]. Importantly, radiation-induced lymphocyte count reduction and subsequent lymphocyte infiltration into tumors have an impact on overall survival outcomes [13]. Lymphocytes are heterogeneous populations of T cells, B cells, NK cells, and their subpopulations. These subpopulations exhibit varying responses to radiation doses due to differences in radiosensitivity, maturation stage, homeostasis, and interactions between themselves [15]. Moreover, they play distinct roles in the tumor response and treatment efficacy. NK cells are part of the innate immune system and can either kill tumor cells directly or promote the differentiation of cytotoxic T cells into effective cytotoxic T cells that eliminate tumor cells. NK cells exhibit radioresistance both in vitro and in vivo, even after whole-body irradiation [27]. Therefore, the reduction in NK cell counts following fractionated brain irradiation is likely driven by mechanisms distinct from those affecting other lymphocyte populations.

Brain injury and neuroinflammation may explain the depletion of NK cells after X-ray irradiation. Systemic reductions in NK cell levels have been reported in glioblastoma patients undergoing chemoradiotherapy, primarily due to the secretion of mediators that induce NK cell infiltration [28]. Additionally, during neuroinflammation at the tissue level, NK cell infiltration attracts and regulates neutrophil and monocyte infiltration into the brain through chemokine secretion [29]. The strong correlation observed between NK cells and myeloid subpopulations following X-ray irradiation further supports the existence of neuroinflammation involving the activation of the innate immune system. This finding aligns with previous findings highlighting the activation of innate immune cells by proinflammatory cytokines following irradiation [30]. Following radiochemotherapy treatment of pancreatic cancer, NK cells play a role in the radiation-induced immune response via an interleukin-8–dependent mechanism, and a reduction in circulating NK cells following treatment is associated with poorer overall survival [31].

Our results suggest that brain irradiation induces an increase in the NLR and that proton therapy may prevent long-term increases in the NLR after irradiation. This finding has significant implications for both radiotherapy treatments and future modalities, such as immunotherapy, particularly for multimodal therapeutic approaches. NLR components (neutrophils and lymphocytes) have been identified as important factors for the prognosis of patients receiving radiotherapy. Neutrophils are the most abundant circulating white blood cells and are known for their rapid response to acute inflammation. They play a critical role in initiating and sustaining immune reactions throughout the body [32]. Emerging evidence supports their role in regulating both the innate and adaptive immune systems during tumor development [33]. Studies have shown that neutrophil depletion through anti-Ly6G antibody-mediated effects can enhance the efficacy of radiation therapy [34]. Moreover, retrospective analyses of large patient cohorts have demonstrated a robust correlation between baseline blood neutrophil counts and three-year overall survival rates in patients with various types of cancer [33]. Additionally, an early increase in neutrophil count during irradiation has been associated with higher recurrence rates and reduced survival in patients with cervical cancer [35]. In addition, we demonstrated that the change in the NLR after brain irradiation did not depend on the irradiation volume or dose. This suggests that the systemic inflammation detected by the NLR following brain irradiation was likely due to the systemic response of the body when part of the brain was exposed to radiation, independent of how much and how fast it was irradiated. It is widely documented that radiation causes inflammation in the brain by activating microglia and endothelial cells, which triggers a chain of events that alter the levels of cytokines and chemokines in the brain and perturb the systemic immune system [36].

Our results showed that the LMR and ALC decreased during X-ray irradiation. However, while the ALC fully recovered by day 28, the LMR exhibited poor recovery. Given that both ALC and monocyte levels on day 28 were significantly different from those in the control group, the limited recovery of LMR suggested an interaction between lymphocytes and monocytes following irradiation. This interaction could serve as a more informative marker than examining lymphocyte or monocyte levels alone. High pretreatment monocyte counts and low pretreatment LMR are poor prognostic factors in patients with solid tumors [37,38]. In patients with metastatic renal cell carcinoma treated with immune checkpoint inhibitors, an elevated LMR before treatment initiation and an increase during treatment correlated with improved outcomes [39]. However, there has been limited research on the association between the LMR and the response to radiotherapy. Additionally, whether variations in the LMR following radiotherapy are correlated with treatment efficacy remains unclear. Monocytes, as a type of myeloid subpopulation, play a significant role in the tumor response. Elevated monocyte counts may facilitate cancer progression by recruiting these cells to the tumor microenvironment, where they promote immune suppression and angiogenesis [40]. At the cellular level, circulating lymphocytes and monocytes are sources of tumor-infiltrating lymphocytes (TILs) and tumor-associated macrophages (TAMs), respectively [41,42]. TILs are responsible for mounting anti-tumor immune responses, whereas TAMs play a role in accelerating tumor progression and contributing to immune responses [40,43]. Consequently, a low circulation level may reflect a weakened anti-tumor immune response and a microenvironment conducive to tumor growth. Tracking the LMR after radiotherapy may offer valuable insights into the impact of radiation on the immune system.

In addition, interactions between myeloid and lymphoid lineages have also been described as interactions between lymphocytes and myeloid-derived suppressor cells (MDSCs); in particular, RILs have been shown to be induced by MDSCs. MDSCs constitute a population of immature myeloid cells that includes monocytes and granulocytes, such as neutrophils. MDSCs can indeed exert suppressive effects on various immune effector cells, such as T cells, by inhibiting their proliferation [44] and myelopoiesis. Brain irradiation can increase the levels of circulating MDSCs and further suppress T cells in glioblastoma patients [45]. Glioblastoma mouse models have further shown a cause-and-effect relationship between radiation-induced MDSCs and RILs [45]. Inhibition of MDSCs using pharmaceutical agents has demonstrated promising results in reducing RILs, increasing the presence of TILs, and enhancing the effector functions of T cells in preclinical and clinical settings [45,46]. Finally, the expansion of myeloid cells may underlie the

suppressive effect of radiation on lymphocytes, as suggested by our observations of neutrophilia following irradiation.

Our study illustrated the differences between X-ray and proton therapies in the context of RILs. While RILs induced by X-rays displayed the potential for recovery within 28 days post-irradiation, it coincided with changes in lymphocyte subpopulations, reflecting heterogeneous radiosensitivity. In contrast, proton therapy minimized these subpopulation changes, suggesting an advantage in preserving lymphocyte diversity. The ability of proton therapy to deliver radiation with a smaller entrance dose and negligible exit dose permits the reduction of radiation doses to normal structures. This effect is advantageous for sparing lymphatic organs and circulating blood [21,47], thus effectively mitigating RILs. However, neutrophils have a short lifespan and a high renewal rate [15]. It is also essential to acknowledge that proton therapy may not confer the same benefits to neutrophils owing to their short lifespans and rapid renewal rates. Furthermore, our findings revealed distinctions in the interplay between the leukocyte subpopulations induced by X-rays and protons. These differences suggest divergent systemic effects driven by irradiation type, consistent with previous reports [48,49]. The variations in leukocyte interactions following X-rays and protons suggest a potential dissimilarity in the biological effects of these two irradiation types on the immune system. These findings emphasize the complex interplay between radiation parameters and immune responses, shedding light on how different factors influence leukocyte subpopulations during and after brain irradiation.

Our findings illustrate a correlation between increased irradiated brain volume and decreased dose rate with elevated myeloid cell concentration and reduced lymphoid cell concentration during irradiation. In our earlier investigation, we established that variations in the irradiation volume and dose rate significantly influence early changes in myeloid cell subpopulations following brain irradiation [21]. Additionally, a previous simulation study suggested that higher irradiated brain volume and lower dose rates result in increased blood exposure to radiation [47]. Given their heightened radiosensitivity [50,51], circulating lymphocytes are particularly susceptible to adverse effects when a larger blood volume is exposed to radiation. In addition to X-rays or protons, factors such as dose rate and irradiated brain volume, other radiation-related variables should also be taken into account. Previous research has indicated that the configuration of dynamic beam delivery affects the radiation dose absorbed by circulating blood, even when the fractionated dose and dose rate remain constant [52].

There were species differences between the results from studies on tumor-free rodents and the clinical context of brain cancer patients undergoing radiotherapy. Research involving glioblastoma patients revealed prolonged

radiation-induced lymphopenia without recovery for months following radiotherapy [19,53]. This finding contrasts with our findings, where changes in lymphocyte subpopulations during brain irradiation recovered within one month. In fact, glioblastoma itself can create an immunosuppressive environment at the systemic level and cause lymphopenia [54], independent of cancer treatment. Therefore, the discrepancy in lymphopenia recovery observed in our studies compared to clinical data could be due to the absence of the tumor. For this reason, it is crucial to understand the effects of radiation-induced lymphopenia and its recovery in tumor-free individuals, as it reflects the isolated impact of radiotherapy on systemic immunity. To prevent long-term lymphopenia, the focus should be more on controlling the tumor rather than modifying the treatment to avoid lymphopenia. Furthermore, the greater thymic output of newly matured lymphocytes in rodents than in humans could also partly explain the more rapid recovery observed in mice [55].

5 Conclusion

A tumor-free experimental model was used to isolate the effects of brain radiotherapy on systemic immunity, given the complex interactions between the tumor microenvironment, systemic immunity and radiotherapy. Using fractionated irradiation with a total dose of 20 Gy delivered by a vertical beam to either the whole brain or hemi-brain, proton irradiation induces fewer adverse effects on the immune system compared to X-rays in tumor-free rodents. Both X-ray and proton brain irradiation influenced systemic inflammation, as evidenced by changes in the NLR. X-ray therapy caused an early reduction in ALC and a prolonged increase in NLR, effects that were not observed with proton therapy. Additionally, X-ray brain irradiation delayed the increase in neutrophil levels, whereas neutrophilia induced by proton therapy reduced post-irradiation. At the lymphocyte subpopulation level, X-ray brain irradiation impacted not only the total lymphocyte count but also the proportions of lymphocyte subpopulations. This effect was mitigated with proton irradiation. These findings may be relevant to combining radiotherapy with immunotherapy. However, due to interspecies differences between humans and rodents and the absence of tumors in this study, further research is needed to confirm and understand the mechanisms behind the potential benefits of proton therapy in brain irradiation.

List of abbreviations

NLR	Neutrophil-to-lymphocyte ratio
ALC	Absolute lymphocyte count

LMR	Lymphocyte-monocyte ratio
RIL	Radiation-induced lymphopenia
PCA	Principal component analysis
AIC	Akaike information criterion
MSE	Mean squared error
TILs	Tumor-infiltrating lymphocytes
TAMs	Tumor-associated macrophages
MDSC	Myeloid-derived suppressor cells

Declarations

Ethics approval and consent to participate

Not applicable.

Consent for publication

Not applicable.

Availability of data and material

All other data will be made available upon reasonable request made to the corresponding author upon reasonable request.

Competing interests

The authors declare no conflicts of interest.

Funding

This project received financial support from the CNRS through the 80|Prime program and Ligue Contre le Cancer.

Authors' contributions

TP, JC, JT, and SV conducted the *in vivo* experiments. TP, JT, and SV designed the protocol and analyzed the data. TP, JT, and SV wrote and edited the paper. All authors approved the final version of the paper.

Acknowledgments

Not applicable.

Reference

[1] C.S.D. Roxburgh, D.C. McMillan, Cancer and systemic inflammation: treat the tumour and treat the host, Br J Cancer 110 (2014) 1409–1412. https://doi.org/10.1038/bjc.2014.90.

[2] X.-B. Gu, T. Tian, X.-J. Tian, X.-J. Zhang, Prognostic significance of neutrophil-to-lymphocyte ratio in non-small cell lung cancer: a meta-analysis, Sci Rep 5 (2015) 12493. https://doi.org/10.1038/srep12493.

[3] M. Capone, D. Giannarelli, D. Mallardo, G. Madonna, L. Festino, A.M. Grimaldi, V. Vanella, E. Simeone, M. Paone, G. Palmieri, E. Cavalcanti, C. Caracò, P.A. Ascierto, Baseline neutrophil-to-lymphocyte ratio (NLR) and derived NLR could predict overall survival in patients with advanced melanoma treated with nivolumab, J. Immunotherapy Cancer 6 (2018) 74. https://doi.org/10.1186/s40425-018-0383-1.

[4] A. Buonacera, B. Stancanelli, M. Colaci, L. Malatino, Neutrophil to Lymphocyte Ratio: An Emerging Marker of the Relationships between the Immune System and Diseases, IJMS 23 (2022) 3636. https://doi.org/10.3390/ijms23073636.

[5] H. Peng, X. Luo, Prognostic significance of elevated pretreatment systemic inflammatory markers for patients with prostate cancer: a meta-analysis, Cancer Cell Int 19 (2019) 70. https://doi.org/10.1186/s12935-019-0785-2.

[6] Z. Wang, P. Zhan, Y. Lv, K. Shen, Y. Wei, H. Liu, Y. Song, Prognostic role of pretreatment neutrophil-to-lymphocyte ratio in non-small cell lung cancer patients treated with systemic therapy: a meta-analysis, Transl. Lung Cancer Res 8 (2019) 214–226. https://doi.org/10.21037/tlcr.2019.06.10.

[7] C.I. Yoon, D. Kim, S.G. Ahn, S.J. Bae, C. Cha, S. Park, S. Park, S.I. Kim, H.S. Lee, J.Y. Park, J. Jeong, Radiotherapy-Induced High Neutrophil-to-Lymphocyte Ratio is a Negative Prognostic Factor in Patients with Breast Cancer, Cancers 12 (2020) 1896. https://doi.org/10.3390/cancers12071896.

[8] M. Mason, C. Maurice, M.G. McNamara, M.T. Tieu, Z. Lwin, B.-A. Millar, C. Menard, N. Laperriere, M. Milosevic, E.G. Atenafu, W. Mason, C. Chung, Neutrophil–lymphocyte ratio dynamics during concurrent chemo-radiotherapy for glioblastoma is an independent predictor for overall survival, J Neurooncol 132 (2017) 463–471. https://doi.org/10.1007/s11060-017-2395-y.

[9] Y. Ma, J. Zhang, X. Chen, Lymphocyte-to-Monocyte Ratio is Associated with the Poor Prognosis of Breast Cancer Patients Receiving Neoadjuvant Chemotherapy, CMAR Volume 13 (2021) 1571–1580. https://doi.org/10.2147/CMAR.S292048.

[10] D. Heylmann, V. Ponath, T. Kindler, B. Kaina, Comparison of DNA repair and radiosensitivity of different blood cell populations, Sci Rep 11 (2021) 2478. https://doi.org/10.1038/s41598-021-81058-1.

[11] M. Cesaire, B. Le Mauff, A. Rambeau, O. Toutirais, J. Thariat, Mécanismes de la lymphopénie radio-induite et implications thérapeutiques, Bulletin du Cancer 107 (2020) 813–822. https://doi.org/10.1016/j.bulcan.2020.04.009.

[12] C. Terrones-Campos, B. Ledergerber, I.R. Vogelius, M. Helleberg, L. Specht, J. Lundgren, Hematological toxicity in patients with solid malignant tumors treated with radiation – Temporal analysis, dose response and impact on survival, Radiotherapy and Oncology 158 (2021) 175–183. https://doi.org/10.1016/j.radonc.2021.02.029.

[13] B.P. Venkatesulu, S. Mallick, S.H. Lin, S. Krishnan, A systematic review of the influence of radiation-induced lymphopenia on survival outcomes in solid tumors, Critical Reviews in Oncology/Hematology 123 (2018) 42–51. https://doi.org/10.1016/j.critrevonc.2018.01.003.

[14] E. Velardi, J.J. Tsai, M.R.M. van den Brink, T cell regeneration after immunological injury, Nat Rev Immunol 21 (2021) 277–291. https://doi.org/10.1038/s41577-020-00457-z.

[15] T.-N. Pham, J. Coupey, S. Valable, J. Thariat, S. Valable, Lymphocyte radiosensitivity: a substitution model to the linear-quadratic model?, Int J Radiat Oncol Biol Phys Sous révision (2024).

[16] M. Mangel, M.B. Bonsall, Stem cell biology is population biology: differentiation of hematopoietic multipotent progenitors to common lymphoid and myeloid progenitors, Theor Biol Med Model 10 (2013) 5. https://doi.org/10.1186/1742-4682-10-5.

[17] P. Fang, Y. Shiraishi, V. Verma, W. Jiang, J. Song, B.P. Hobbs, S.H. Lin, Lymphocyte-Sparing Effect of Proton Therapy in Patients with Esophageal Cancer Treated with Definitive Chemoradiation, International Journal of Particle Therapy 4 (2017) 23–32. https://doi.org/10.14338/IJPT-17-00033.1.

[18] D.M. Routman, T.J. Whitaker, C.N. Day, W.S. Harmsen, M.A. Neben-Wittich, M.G. Haddock, C.L. Hallemeier, K. Merrell, Predictors of lymphopenia in esophageal cancer patients receiving photon or proton radiation therapy: A dosimetric analysis., JCO 37 (2019) 147–147. https://doi.org/10.1200/JCO.2019.37.4_suppl.147.

[19] R. Mohan, A.Y. Liu, P.D. Brown, A. Mahajan, J. Dinh, C. Chung, S. McAvoy, M.F. McAleer, S.H. Lin, J. Li, A.J. Ghia, C. Zhu, E.P. Sulman, J.F. de Groot, A.B. Heimberger, S.L. McGovern, C. Grassberger, H. Shih, S. Ellsworth, D.R. Grosshans, Proton therapy reduces the likelihood of high-grade radiation-induced lymphopenia in glioblastoma

patients: phase II randomized study of protons vs photons, Neuro-Oncology 23 (2021) 284–294. https://doi.org/10.1093/neuonc/noaa182.
[20] J. Coupey, T.N. Pham, J. Toutain, V. Ivanova, E. HUE, C. Helaine, A. Ismail, R. Saulnier, G. Simonin, M. Rousseau, C. Moignier, J. Thariat, S. Valable, Investigating the effects of protons versus x-rays on radiation-induced lymphopenia after brain irradiation, bioRxiv (2024). https://doi.org/10.1101/2024.03.02.583088.
[21] T.-N. Pham, J. Coupey, J. Toutain, S.M. Candeias, G. Simonin, M. Rousseau, O. Touzani, J. Thariat, S. Valable, Early effects of different brain radiotherapy modalities on circulating leucocyte subpopulations in rodents, International Journal of Radiation Biology (2024) 1–12. https://doi.org/10.1080/09553002.2024.2324471.
[22] J. Constanzo, M. Vanstalle, C. Finck, D. Brasse, M. Rousseau, Dosimetry and characterization of a 25-MeV proton beam line for preclinical radiobiology research, Medical Physics 46 (2019) 2356–2362. https://doi.org/10.1002/mp.13512.
[23] R. Kolde, Pretty Heatmaps, (2022).
[24] S. Lê, J. Josse, F. Husson, **FactoMineR** : An *R* Package for Multivariate Analysis, J. Stat. Soft. 25 (2008). https://doi.org/10.18637/jss.v025.i01.
[25] P. Lissoni, S. Meregalli, S. Curreri, G. Messina, F. Brivio, L. Fumagalli, M. Colciago, G. Gardani, Brain Irradiation-Induced Lymphocytosis Predicts Response in Cancer Patients with Brain Metastases, Int J Biol Markers 23 (2008) 111–114. https://doi.org/10.1177/172460080802300207.
[26] T.H. So, S.K. Chan, W.L. Chan, H. Choi, C.L. Chiang, V. Lee, T.C. Lam, I. Wong, S. Law, D. Kwong, F. Ming (Spring) Kong, J.Y. Jin, K.O. Lam, Lymphopenia and Radiation Dose to Circulating Lymphocytes With Neoadjuvant Chemoradiation in Esophageal Squamous Cell Carcinoma, Advances in Radiation Oncology 5 (2020) 880–888. https://doi.org/10.1016/j.adro.2020.03.021.
[27] H.-R. Park, U. Jung, Depletion of NK Cells Resistant to Ionizing Radiation Increases Mutations in Mice After Whole-body Irradiation, In Vivo 35 (2021) 1507–1513. https://doi.org/10.21873/invivo.12403.
[28] C.E. Fadul, J.L. Fisher, J. Gui, T.H. Hampton, A.L. Cote, M.S. Ernstoff, Immune modulation effects of concomitant temozolomide and radiation therapy on peripheral blood mononuclear cells in patients with glioblastoma multiforme, Neuro-Oncology 13 (2011) 393–400. https://doi.org/10.1093/neuonc/noq204.
[29] H. He, T. Geng, P. Chen, M. Wang, J. Hu, L. Kang, W. Song, H. Tang, NK cells promote neutrophil recruitment in the brain during sepsis-induced neuroinflammation, Sci Rep 6 (2016) 27711. https://doi.org/10.1038/srep27711.
[30] S.A. Lorimore, J.A. Chrystal, J.I. Robinson, P.J. Coates, E.G. Wright, Chromosomal Instability in Unirradiated Hemaopoietic Cells Induced by Macrophages Exposed *In vivo* to Ionizing Radiation, Cancer Research 68 (2008) 8122–8126. https://doi.org/10.1158/0008-5472.CAN-08-0698.
[31] T. Walle, J.A. Kraske, B. Liao, B. Lenoir, C. Timke, E. Von Bohlen Und Halbach, F. Tran, P. Griebel, D. Albrecht, A. Ahmed, M. Suarez-Carmona, A. Jiménez-Sánchez, T. Beikert, A. Tietz-Dahlfuß, A.N. Menevse, G. Schmidt, M. Brom, J.H.W. Pahl, W. Antonopoulos, M. Miller, R.L. Perez, F. Bestvater, N.A. Giese, P. Beckhove, P. Rosenstiel, D. Jäger, O. Strobel, D. Pe'er, N. Halama, J. Debus, A. Cerwenka, P.E. Huber, Radiotherapy orchestrates natural killer cell dependent antitumor immune responses through CXCL8, Sci. Adv. 8 (2022) eabh4050. https://doi.org/10.1126/sciadv.abh4050.
[32] H.L. Malech, F.R. DeLeo, M.T. Quinn, The Role of Neutrophils in the Immune System: An Overview, in: M.T. Quinn, F.R. DeLeo (Eds.), Neutrophil Methods and Protocols, Humana Press, Totowa, NJ, 2014: pp. 3–10. https://doi.org/10.1007/978-1-62703-845-4_1.
[33] A. Schernberg, P. Blanchard, C. Chargari, E. Deutsch, Neutrophils, a candidate biomarker and target for radiation therapy?, Acta Oncologica 56 (2017) 1522–1530. https://doi.org/10.1080/0284186X.2017.1348623.
[34] G.-O. Ahn, D. Tseng, C.-H. Liao, M.J. Dorie, A. Czechowicz, J.M. Brown, Inhibition of Mac-1 (CD11b/CD18) enhances tumor response to radiation by reducing myeloid cell recruitment, Proc. Natl. Acad. Sci. U.S.A. 107 (2010) 8363–8368. https://doi.org/10.1073/pnas.0911378107.
[35] A.J. Wisdom, C.S. Hong, A.J. Lin, Y. Xiang, D.E. Cooper, J. Zhang, E.S. Xu, H.-C. Kuo, Y.M. Mowery, D.J. Carpenter, K.T. Kadakia, J.E. Himes, L. Luo, Y. Ma, N. Williams, D.M. Cardona, M. Haldar, Y. Diao, S. Markovina, J.K. Schwarz, D.G. Kirsch, Neutrophils promote tumor resistance to radiation therapy, Proc. Natl. Acad. Sci. U.S.A. 116 (2019) 18584–18589. https://doi.org/10.1073/pnas.1901562116.
[36] K. Lumniczky, T. Szatmári, G. Sáfrány, Ionizing Radiation-Induced Immune and Inflammatory Reactions in the Brain, Front. Immunol. 8 (2017) 517. https://doi.org/10.3389/fimmu.2017.00517.
[37] T.F. Nishijima, H.B. Muss, S.S. Shachar, K. Tamura, Y. Takamatsu, Prognostic value of lymphocyte-to-monocyte ratio in patients with solid tumors: A systematic review and meta-analysis, Cancer Treatment Reviews 41 (2015) 971–978. https://doi.org/10.1016/j.ctrv.2015.10.003.

[38] S. Wen, N. Chen, Y. Hu, L. Huang, J. Peng, M. Yang, X. Shen, Y. Song, L. Xu, Elevated peripheral absolute monocyte count related to clinicopathological features and poor prognosis in solid tumors: Systematic review, meta-analysis, and meta-regression, Cancer Medicine 10 (2021) 1690–1714. https://doi.org/10.1002/cam4.3773.

[39] M.A. Bilen, D.J. Martini, Y. Liu, C. Lewis, H.H. Collins, J.M. Shabto, M. Akce, H.T. Kissick, B.C. Carthon, W.L. Shaib, O.B. Alese, R.N. Pillai, C.E. Steuer, C.S. Wu, D.H. Lawson, R.R. Kudchadkar, B.F. El-Rayes, V.A. Master, S.S. Ramalingam, T.K. Owonikoko, R.D. Harvey, The prognostic and predictive impact of inflammatory biomarkers in patients who have advanced-stage cancer treated with immunotherapy: Inflammatory Biomarkers in Immunotherapy, Cancer 125 (2019) 127–134. https://doi.org/10.1002/cncr.31778.

[40] T. Chanmee, P. Ontong, K. Konno, N. Itano, Tumor-Associated Macrophages as Major Players in the Tumor Microenvironment, Cancers 6 (2014) 1670–1690. https://doi.org/10.3390/cancers6031670.

[41] R. Verma, A.M. Hanby, K. Horgan, E.T. Verghese, M. Volpato, C.R. Carter, T.A. Hughes, Levels of different subtypes of tumour-infiltrating lymphocytes correlate with each other, with matched circulating lymphocytes, and with survival in breast cancer, Breast Cancer Res Treat 183 (2020) 49–59. https://doi.org/10.1007/s10549-020-05757-5.

[42] M. Kiss, S. Van Gassen, K. Movahedi, Y. Saeys, D. Laoui, Myeloid cell heterogeneity in cancer: not a single cell alike, Cellular Immunology 330 (2018) 188–201. https://doi.org/10.1016/j.cellimm.2018.02.008.

[43] Y. Man, A. Stojadinovic, J. Mason, I. Avital, A. Bilchik, B. Bruecher, M. Protic, A. Nissan, M. Izadjoo, X. Zhang, A. Jewett, Tumor-Infiltrating Immune Cells Promoting Tumor Invasion and Metastasis: Existing Theories, J. Cancer 4 (2013) 84–95. https://doi.org/10.7150/jca.5482.

[44] P. Ma, P.L. Beatty, J. McKolanis, R. Brand, R.E. Schoen, O.J. Finn, Circulating Myeloid Derived Suppressor Cells (MDSC) That Accumulate in Premalignancy Share Phenotypic and Functional Characteristics With MDSC in Cancer, Front. Immunol. 10 (2019) 1401. https://doi.org/10.3389/fimmu.2019.01401.

[45] S. Ghosh, J. Huang, M. Inkman, J. Zhang, S. Thotala, E. Tikhonova, N. Miheecheva, F. Frenkel, R. Ataullakhanov, X. Wang, D. DeNardo, D. Hallahan, D. Thotala, Radiation-induced circulating myeloid-derived suppressor cells induce systemic lymphopenia after chemoradiotherapy in patients with glioblastoma, Sci. Transl. Med. 15 (2023) eabn6758. https://doi.org/10.1126/scitranslmed.abn6758.

[46] K.N. Kodumudi, A. Weber, A.A. Sarnaik, S. Pilon-Thomas, Blockade of Myeloid-Derived Suppressor Cells after Induction of Lymphopenia Improves Adoptive T Cell Therapy in a Murine Model of Melanoma, The Journal of Immunology 189 (2012) 5147–5154. https://doi.org/10.4049/jimmunol.1200274.

[47] A. Hammi, H. Paganetti, C. Grassberger, 4D blood flow model for dose calculation to circulating blood and lymphocytes, Phys. Med. Biol. 65 (2020) 055008. https://doi.org/10.1088/1361-6560/ab6c41.

[48] M. Lupu-Plesu, A. Claren, S. Martial, P.-D. N'Diaye, K. Lebrigand, N. Pons, D. Ambrosetti, I. Peyrottes, J. Feuillade, J. Hérault, M. Dufies, J. Doyen, G. Pagès, Effects of proton versus photon irradiation on (lymph)angiogenic, inflammatory, proliferative and anti-tumor immune responses in head and neck squamous cell carcinoma, Oncogenesis 6 (2017) e354–e354. https://doi.org/10.1038/oncsis.2017.56.

[49] M. Durante, S. Formenti, Harnessing radiation to improve immunotherapy: better with particles?, BJR 93 (2020) 20190224. https://doi.org/10.1259/bjr.20190224.

[50] N. Nakamura, Y. Kusunoki, M. Akiyama, Radiosensitivity of CD4 or CD8 positive human T-lymphocytes by an in vitro colony formation assay, Radiat Res 123 (1990) 224–227.

[51] H. Paganetti, A review on lymphocyte radiosensitivity and its impact on radiotherapy, Front. Oncol. 13 (2023) 1201500. https://doi.org/10.3389/fonc.2023.1201500.

[52] A. Hammi, 4D dosimetric-blood flow model: impact of prolonged fraction delivery times of IMRT on the dose to the circulating lymphocytes, Phys. Med. Biol. 68 (2023) 145017. https://doi.org/10.1088/1361-6560/acdcdc.

[53] S.A. Grossman, S. Ellsworth, J. Campian, A.T. Wild, J.M. Herman, D. Laheru, M. Brock, A. Balmanoukian, X. Ye, Survival in Patients With Severe Lymphopenia Following Treatment With Radiation and Chemotherapy for Newly Diagnosed Solid Tumors, J Natl Compr Canc Netw 13 (2015) 1225–1231. https://doi.org/10.6004/jnccn.2015.0151.

[54] R. Domenis, D. Cesselli, B. Toffoletto, E. Bourkoula, F. Caponnetto, I. Manini, A.P. Beltrami, T. Ius, M. Skrap, C. Di Loreto, G. Gri, Systemic T Cells Immunosuppression of Glioma Stem Cell-Derived Exosomes Is Mediated by Monocytic Myeloid-Derived Suppressor Cells, PLoS ONE 12 (2017) e0169932. https://doi.org/10.1371/journal.pone.0169932.

[55] I. den Braber, T. Mugwagwa, N. Vrisekoop, L. Westera, R. Mögling, A. Bregje de Boer, N. Willems, E.H.R. Schrijver, G. Spierenburg, K. Gaiser, E. Mul, S.A. Otto, A.F.C. Ruiter, M.T. Ackermans, F. Miedema, J.A.M. Borghans, R.J. de Boer, K. Tesselaar, Maintenance of Peripheral Naive T Cells Is Sustained by Thymus Output in Mice but Not Humans, Immunity 36 (2012) 288–297. https://doi.org/10.1016/j.immuni.2012.02.006.

Figure

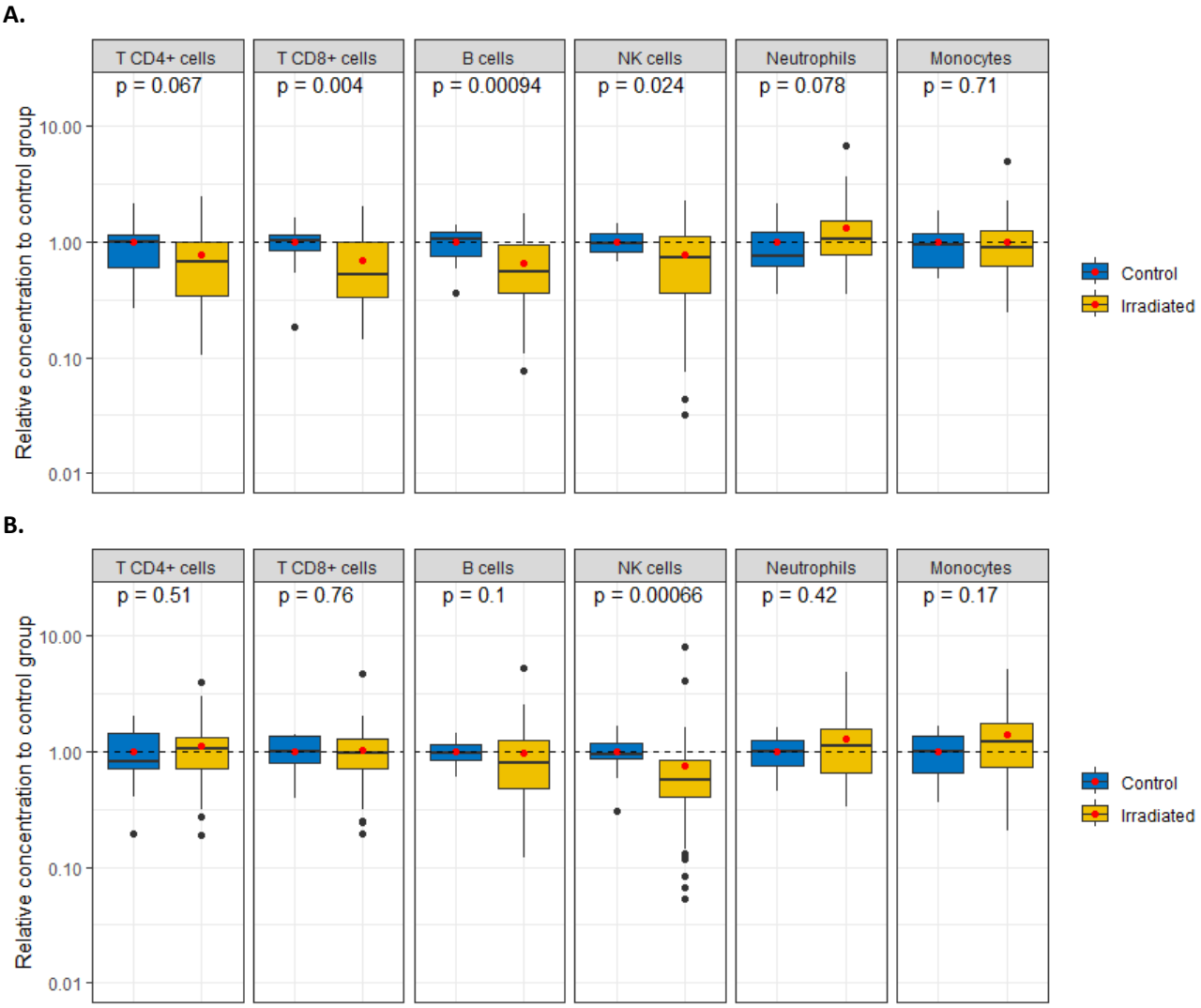

Figure 1. Leukocyte subpopulation levels during irradiation on day 2 (A) and late after irradiation on day 28 (B) in mice (n=16 for control and n=80 for irradiated groups: n=10 * 2 irradiation type (X-rays or protons) * 2 volumes (whole brain or hemi brain) * 2 dose rates (1 Gy/min or 2 Gy/min)). The red points represent the means of the data. Comparisons between control and irradiated mice for each cell subpopulation were performed using the Wilcoxon test.

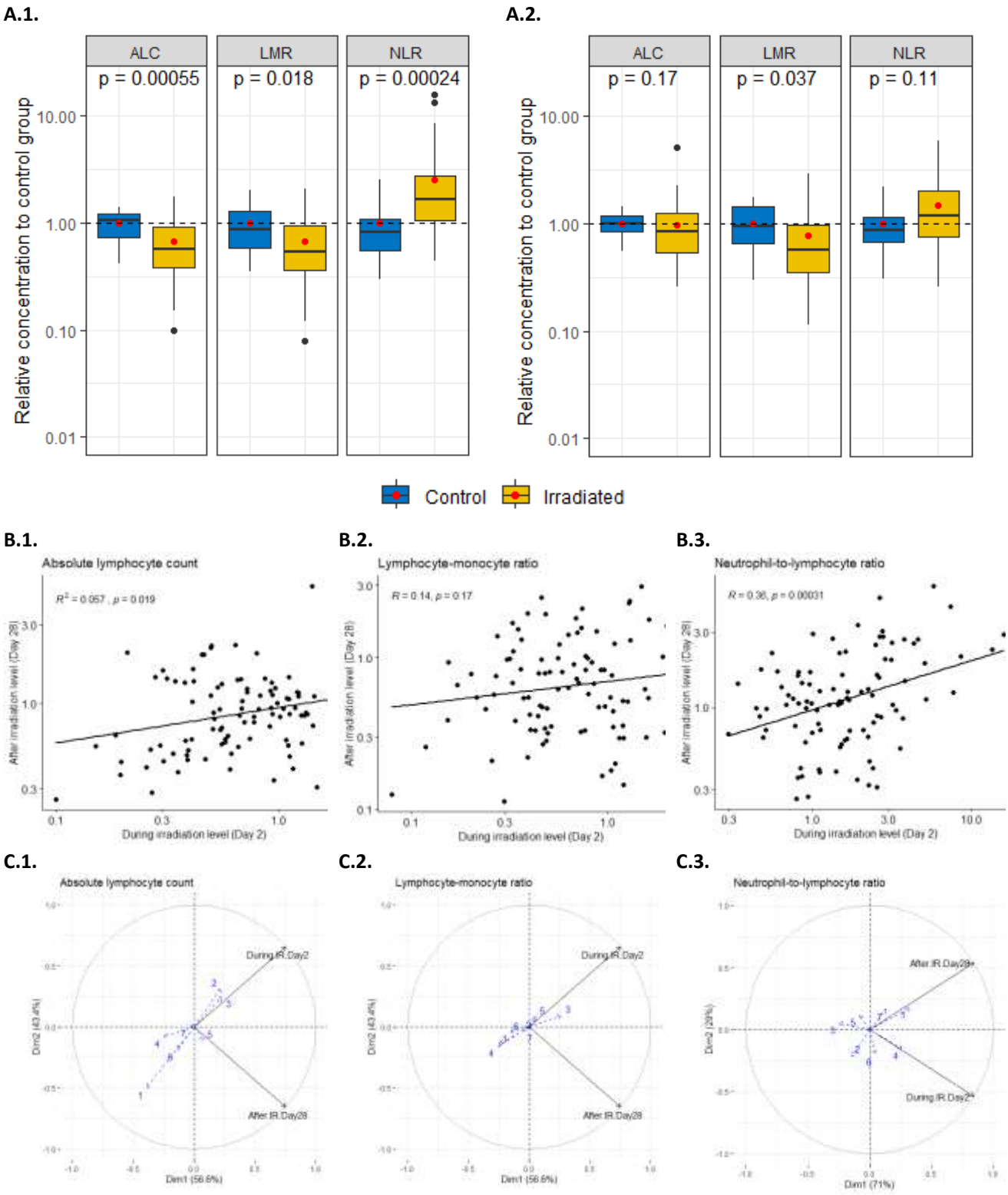

1. X-rays 2. Protons 3. Control (Non-irradiated) 4. Whole brain irradiation 5. Hemi-brain irradiation 6. Dose rate of 1 Gy/min 7. Dose rate of 2 Gy/min

Figure 2. (A) ALC, LMR, and NLR variations under brain irradiation compared with those in the control group. Red points represent the mean values of the data. (B) Correlations between ALC (B.1), LMR (B.2), and NLR (B.3) during irradiation on day 2 and after irradiation on day 28. (C) Principal component analysis of leukocyte-based inflammatory biomarkers, including ALC (C.1), LMR (C.2), and NLR (C.3), during irradiation on day 2 and after

irradiation on day 28 according to the radiation parameters. The blue arrow and text indicate the impact of radiation parameters, including irradiation type (X-rays, protons, or control group), irradiated volume (whole brain or hemi-brain (hemispheres)), and dose rate (1 Gy/min or 2 Gy/min). Comparisons between control and irradiated mice for each leukocyte-based inflammatory biomarker were performed using the Wilcoxon test.

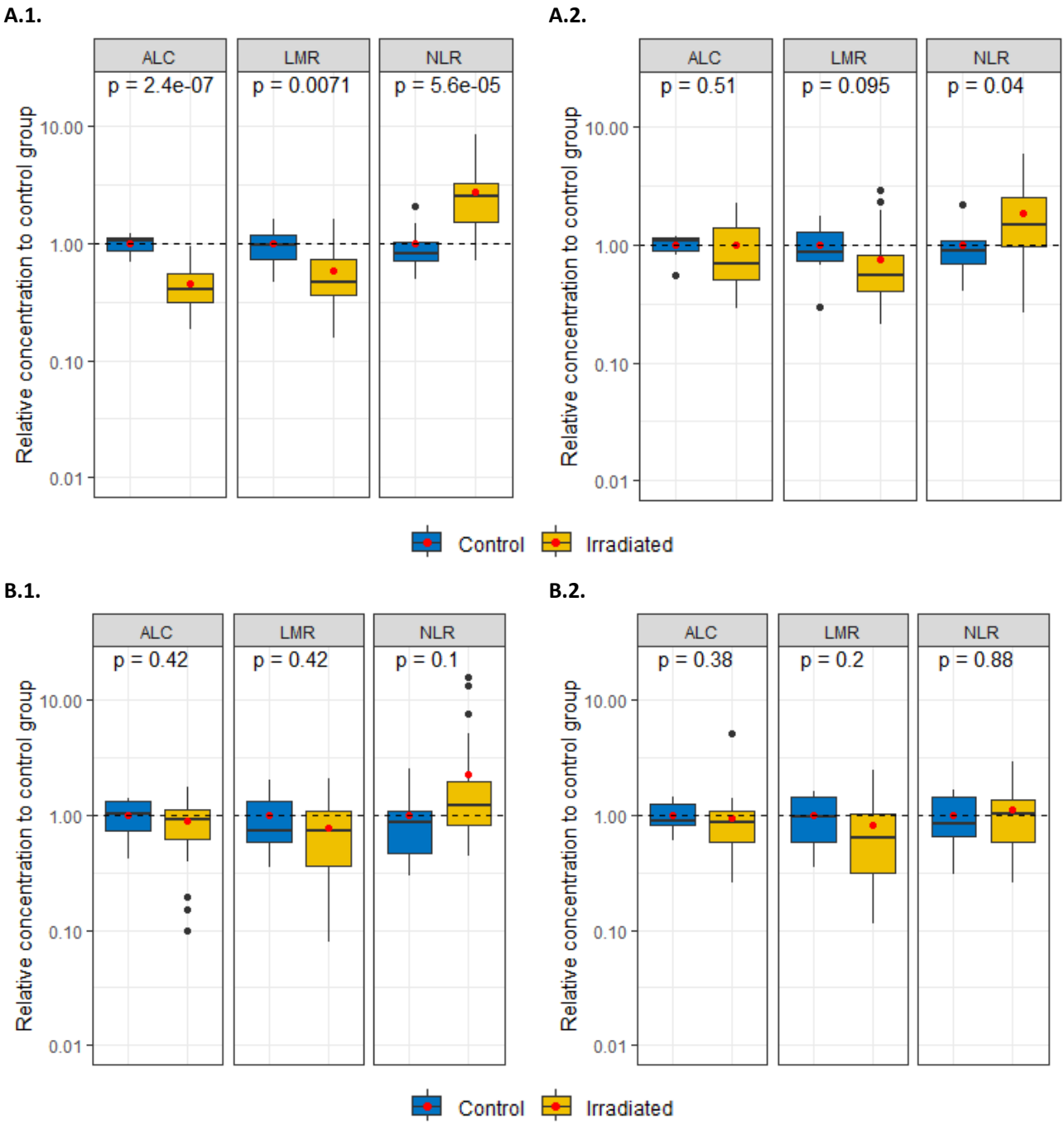

Figure 3. Leukocyte-based inflammatory biomarkers (ALC, LMR, NLR) stratified by irradiation type: (A) X-rays, including (A.1) during irradiation on day 2, (A.2) after irradiation on day 28, and (B) protons, including (B.1) during irradiation on day 2 and (B.2) after irradiation on day 28. Red points represent the mean values of the data. Comparisons between control and irradiated mice for each leukocyte-based inflammatory biomarker were performed using the Wilcoxon test.

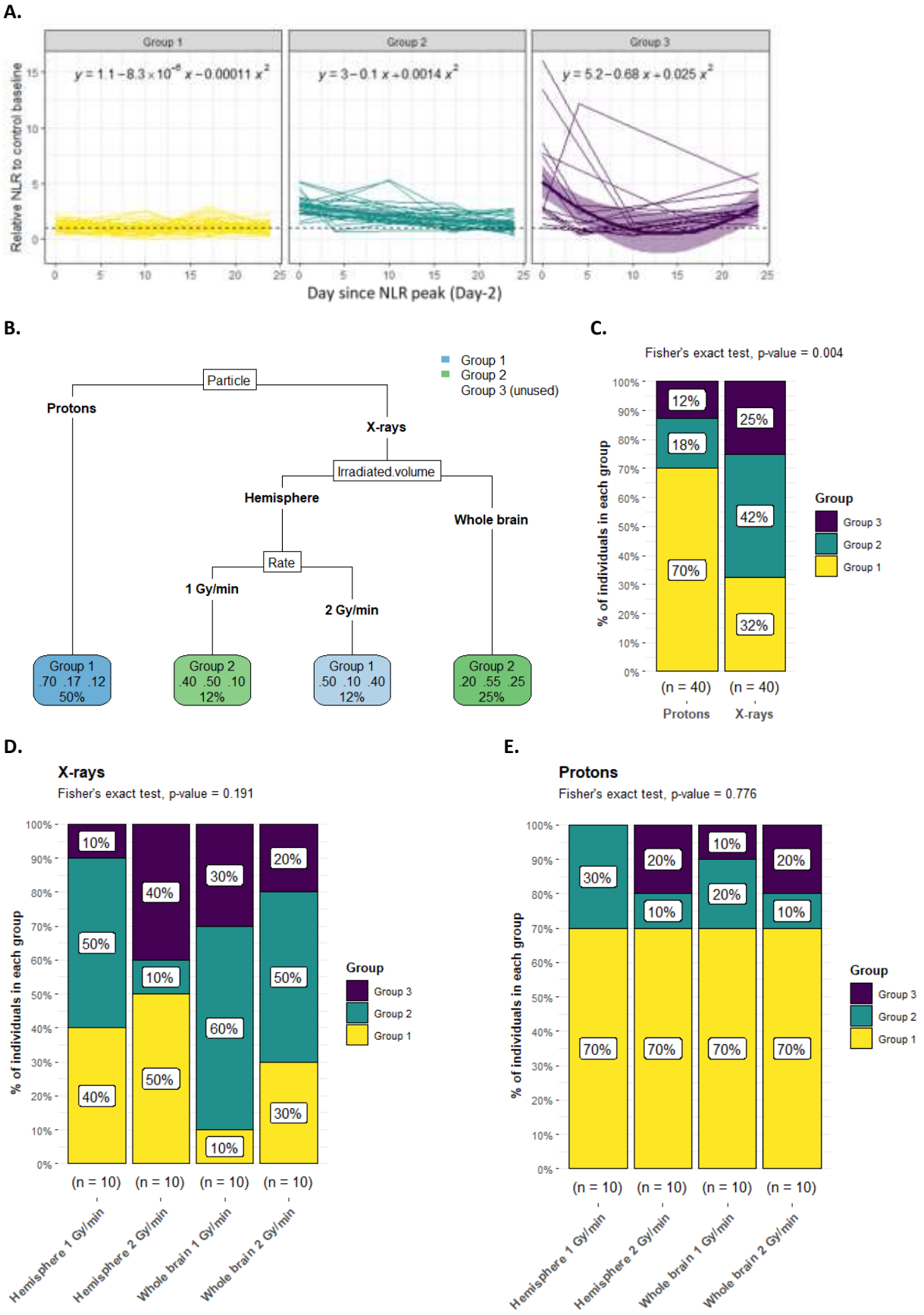

Figure 4. Neutrophil-to-lymphocyte ratio kinetics following brain irradiation. (A) Three clusters were detected using a 2nd-order polynomial mixture model. (B) Tree-based model for classifying NLR kinetic clusters based on radiation parameters. (C) Proportion of NLR clusters in the X-ray and proton irradiation groups. Proportion of NLR clusters

within X-rays (D) or protons (E) stratified by irradiated volume (whole brain or hemi-brain) and dose rate (1 or 2 Gy/min).

A.

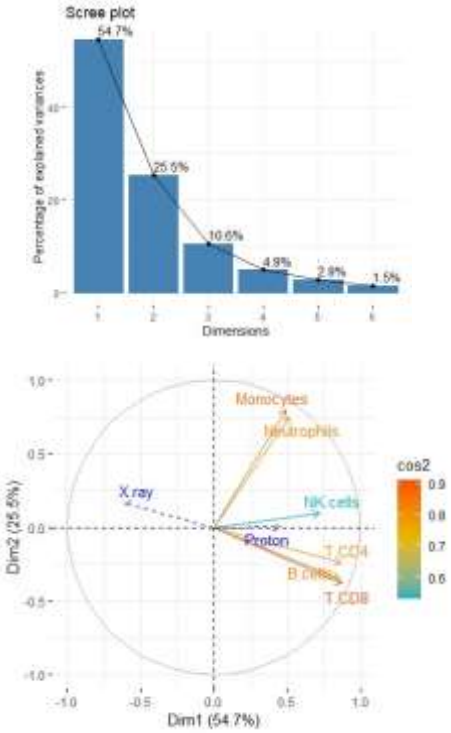

Variable correlation to principal components

	Principal component 1	Principal component 2
T CD4+ cells	0.87	-0.24
T CD8+ cells	0.87	-0.38
B-cells	0.86	-0.35
NK-cells	0.72	0.1
Neutrophils	0.51	0.75
Monocytes	0.49	0.8

Supplementary variable correlation to principal components

	Principal component 1	Principal component 2
Control	0.21	-0.22
X-rays	-0.61	0.17
Protons	0.45	0
Whole-brain	-0.15	0.23
Hemi-brain	-0.01	-0.06
1 Gy/min	-0.15	0.11
2 Gy/min	-0.01	0.06

B.

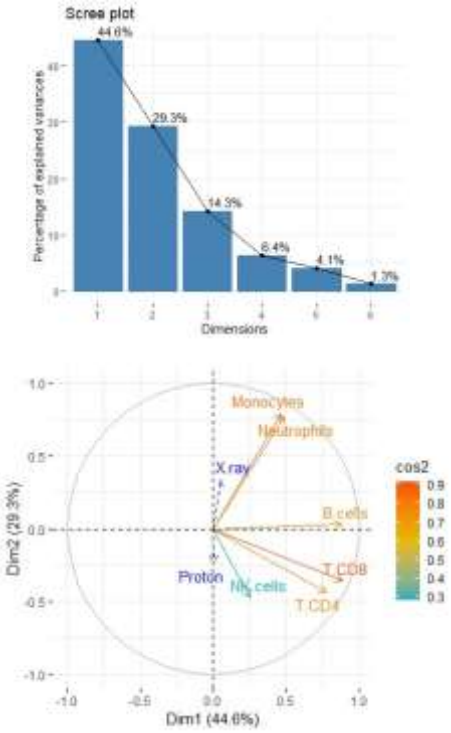

Variable correlation to principal components

	Principal component 1	Principal component 2
T CD4+ cells	0.77	-0.43
T CD8+ cells	0.89	-0.36
B-cells	0.88	0.03
NK-cells	0.25	-0.47
Neutrophils	0.49	0.77
Monocytes	0.46	0.79

Supplementary variable correlation to principal components

	Principal component 1	Principal component 2
Control	-0.07	-0.14
X-rays	0.05	0.34
Protons	0	-0.23
Whole-brain	-0.17	0.13
Hemi-brain	0.23	-0.03
1 Gy/min	0.08	0.02
2 Gy/min	-0.02	0.08

Figure 5. Modifications of leukocyte interplay during irradiation on day 2 (A) and after irradiation on day 28 (B) using principal component analysis. The scree plot represents the percentage of the explained variance for each principal component (dimension). The biplot (round plot) represents the correlation between leukocyte subpopulations (CD4+, T CD8+, B cells, NK cells, neutrophils, and monocytes) and the two principal components. The blue arrow

and text indicate the impact of X-rays, protons, or the control group. The legend “cos2” represents the contributions (on a scale of zero to one) of the variables to the two main principal components.

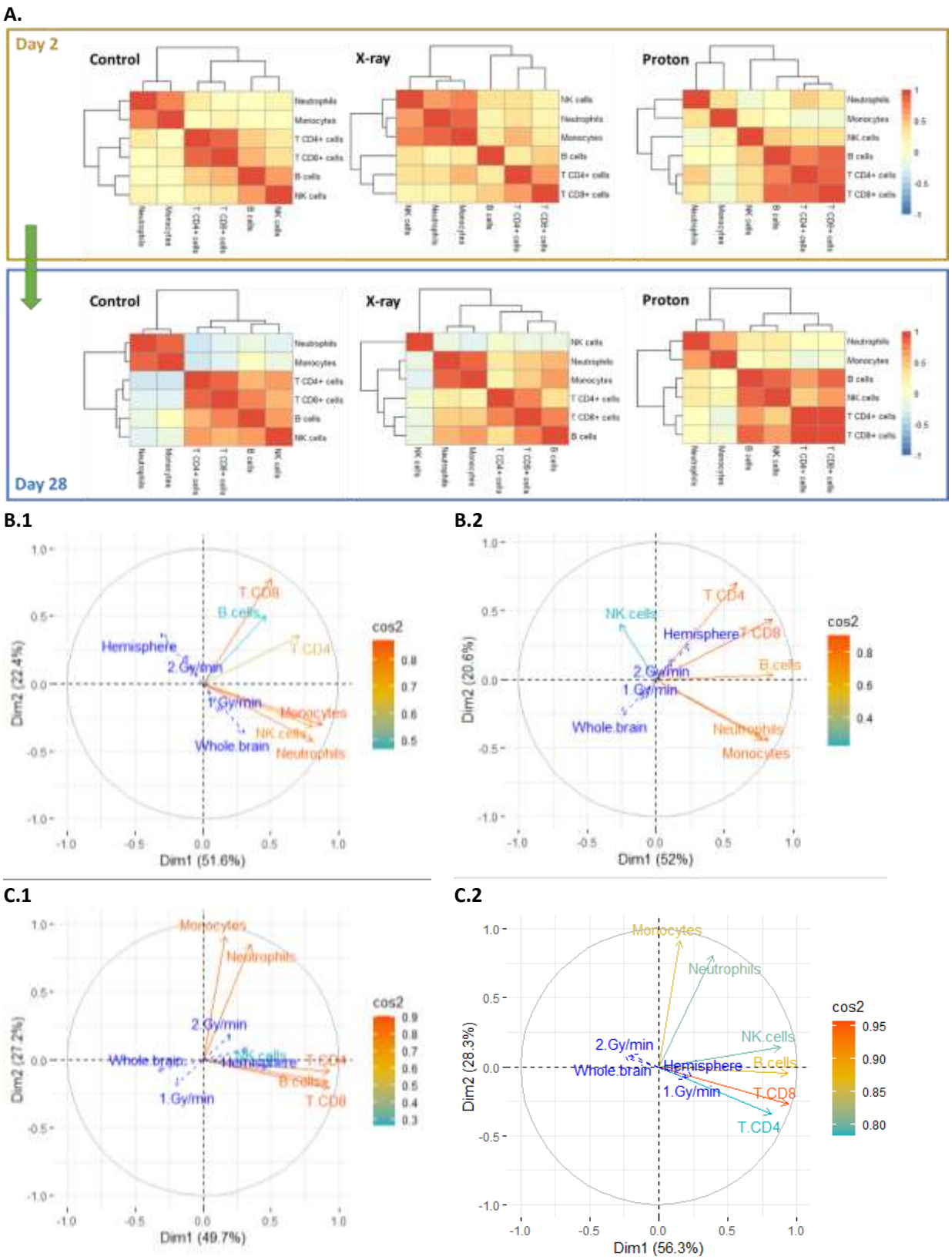

Figure 6. Modifications of leukocyte interplay during and after irradiation stratified by irradiation type: control, X-rays, and protons using (A) correlation analysis and (B, C) principal component analysis of either X-rays (B, including B.1: during irradiation on day 2; and B.2: after irradiation on day 28) or protons (C, including C.1: during irradiation on day 2; and C.2: after irradiation on day 28). The blue arrow and text in the latter figure indicate the impact of

radiation parameters, irradiated volume (whole-brain or hemi-brain (hemisphere)), and dose rate (1 or 2 Gy/min). The legend “cos2” represents the contributions (on a scale of zero to one) of the variables to the two major principal components.

Table

Table 1. Summary of parameters used for analysis

Leukocyte subpopulations	**Leukocyte-based inflammatory** biomarkers	**Radiation-based parameters**
T-CD4+ lymphocytes	Absolute lymphocyte count (ALC)	Beam types: X-rays or protons
T-CD8+ lymphocytes	Neutrophil-to-lymphocyte ratio (NLR)	Irradiated brain volume
B lymphocytes	Monocyte-lymphocyte ratio (MLR)	Dose rate
NK lymphocytes		
Neutrophils		
Monocytes		

Legend: the parameters include 6 leukocyte subpopulations, 3 leukocyte-based inflammatory biomarkers, and radiation-based parameters